Nonequilibrium axial charge production in expanding color fields

Naoto Tanji (ECT*)

Workshop on Chirality, Vorticity and Magnetic Field in Heavy Ion Collisions 2018
March 20th, Galileo Galilei Institute, Firenze

Axial charge production in Glasma

The space-time distribution of axial charges is indispensable for the understanding of CME.

Possible axial charge production mechanisms:

- **Quark production in Glasma**
- Sphaleron transition in QGP/Glasma

Moore, Tassler (2011)
Mace, Schlichting, Venugopalan (2016)

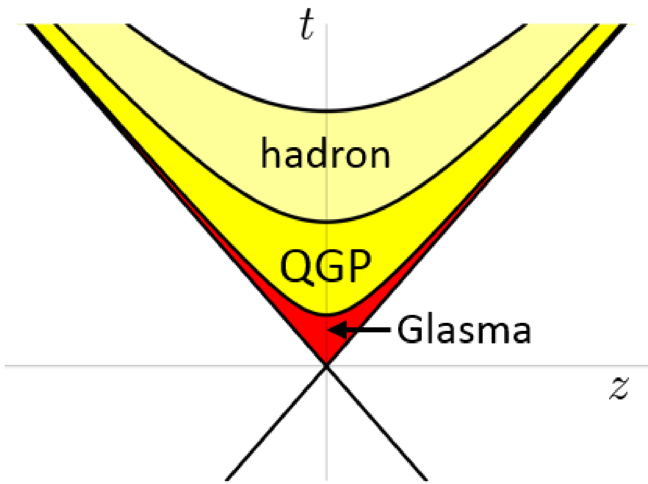

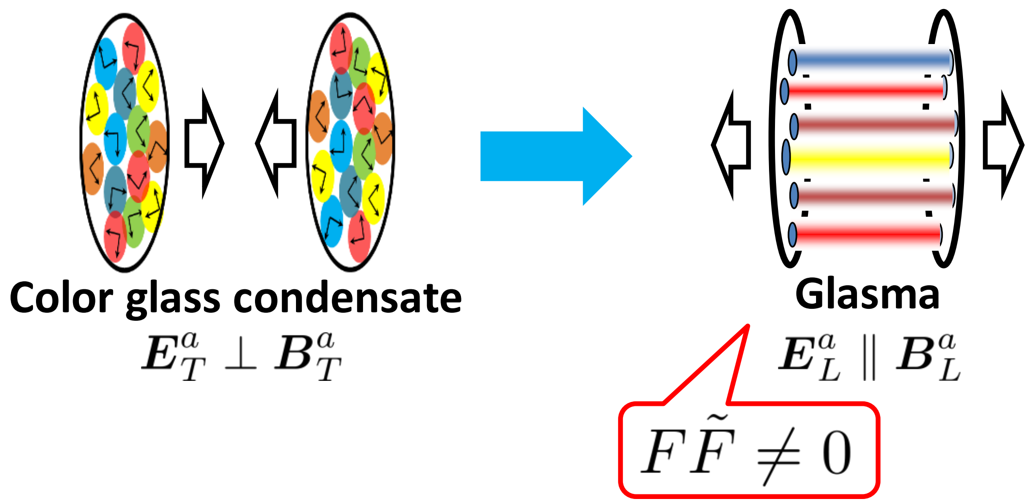

Axial charge production in Glasma

The space-time distribution of axial charges is indispensable for the understanding of CME.

Possible axial charge production mechanisms:

- **Quark production in Glasma**
- Sphaleron transition in QGP/Glasma

Moore, Tassler (2011)
Mace, Schlichting, Venugopalan (2016)

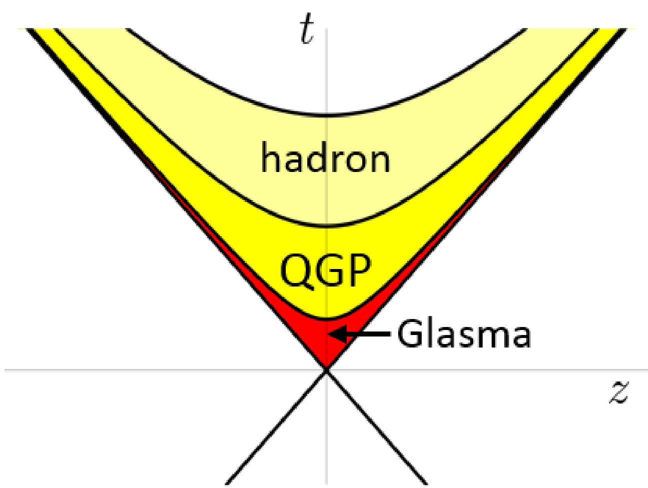

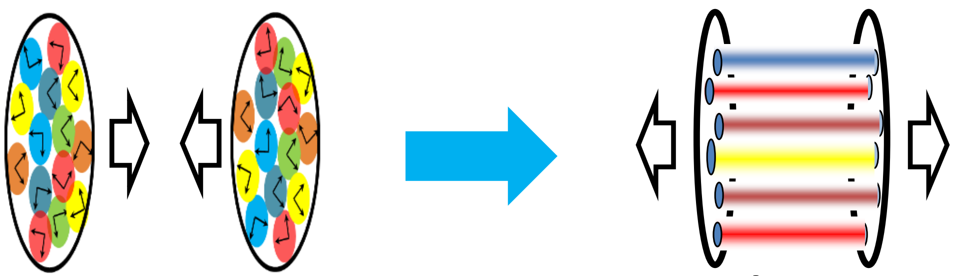

Color glass condensate

$\boldsymbol{E}_T^a \perp \boldsymbol{B}_T^a$

Glasma

$\boldsymbol{E}_L^a \parallel \boldsymbol{B}_L^a$

$\boxed{F\tilde{F} \neq 0}$

Challenges:

Nonequilibrium, Nonperturbative, Quantum dynamics of quarks, Expanding geometry

Real-time lattice simulations of quantum fermion fields and classical gauge fields

CGC initial conditions

Classical YM eqs. coupled to large-x color sources

$$D_\mu F^{\mu\nu} = \delta^{\nu +}\delta(x^-)\rho_{(1)}(\boldsymbol{x}_\perp) + \delta^{\nu -}\delta(x^+)\rho_{(2)}(\boldsymbol{x}_\perp)$$

Solution at $\tau = 0^+$ in the FS gauge $A^\tau = 0$

$$E_z(\tau = 0^+, \boldsymbol{x}_\perp) = -ig\left[\alpha^i_{(1)}, \alpha^i_{(2)}\right]$$
$$B_z(\tau = 0^+, \boldsymbol{x}_\perp) = -ig\epsilon^{ij}\left[\alpha^i_{(1)}, \alpha^j_{(2)}\right]$$

with

$$\alpha^i_{(n)}(\boldsymbol{x}_\perp) = \frac{i}{g} V^\dagger_{(n)} \partial^i V_{(n)}$$
$$V_{(n)}(\boldsymbol{x}_\perp) = \exp\left[-ig\nabla_\perp^{-2}\rho_{(n)}\right]$$

Kovner, McLerran, Weigert (1995)

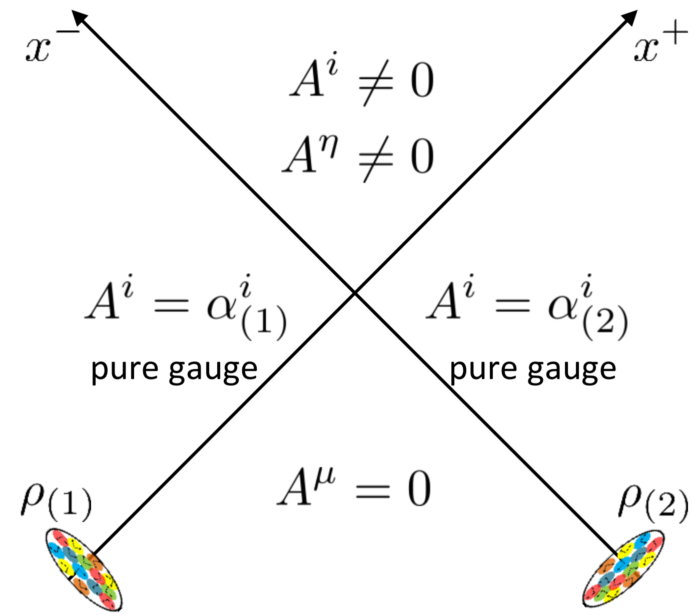

Numerical solution for $\tau > 0$ in the MV model

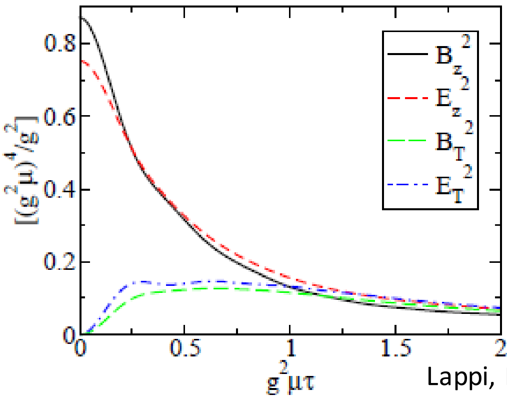

Lappi, McLerran (2006)

CGC initial conditions

Classical YM eqs. coupled to large-x color sources

$$D_\mu F^{\mu\nu} = \delta^{\nu+}\delta(x^-)\rho_{(1)}(\boldsymbol{x}_\perp) + \delta^{\nu-}\delta(x^+)\rho_{(2)}(\boldsymbol{x}_\perp)$$

Solution at $\tau = 0^+$ in the FS gauge $A^\tau = 0$

$$E_z(\tau = 0^+, \boldsymbol{x}_\perp) = -ig\left[\alpha^i_{(1)}, \alpha^i_{(2)}\right]$$
$$B_z(\tau = 0^+, \boldsymbol{x}_\perp) = -ig\epsilon^{ij}\left[\alpha^i_{(1)}, \alpha^j_{(2)}\right]$$

with

$$\alpha^i_{(n)}(\boldsymbol{x}_\perp) = \frac{i}{g}V^\dagger_{(n)}\partial^i V_{(n)}$$
$$V_{(n)}(\boldsymbol{x}_\perp) = \exp\left[-ig\nabla_\perp^{-2}\rho_{(n)}\right]$$

Kovner, McLerran, Weigert (1995)

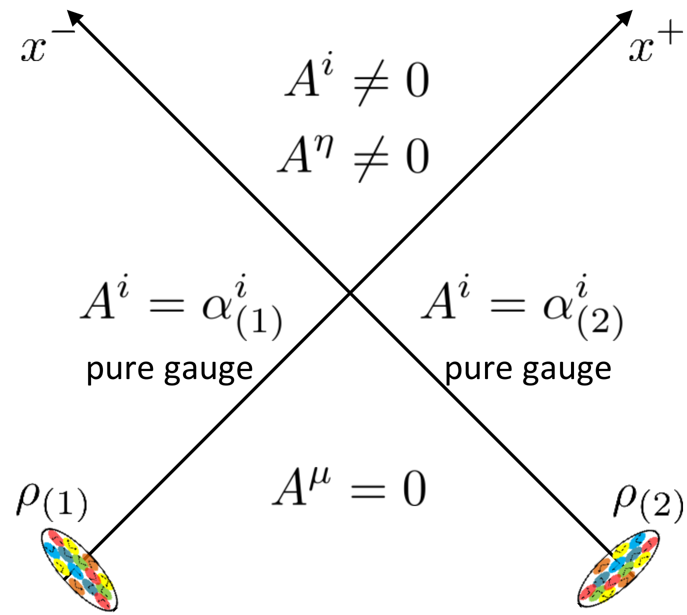

Numerical solution for $\tau > 0$ in the MV model

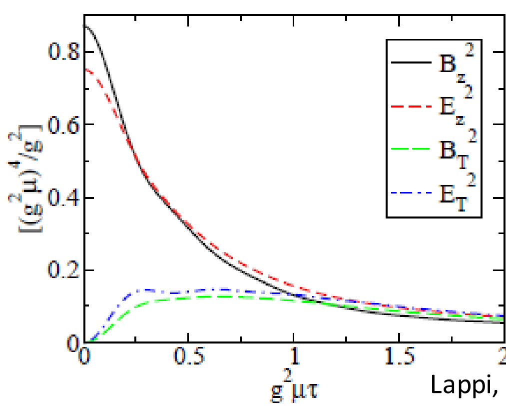

Lappi, McLerran (2006)

We consider flux-tube-like configurations with a Gaussian profile

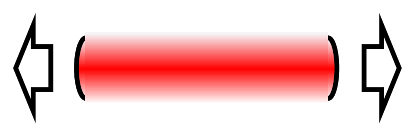

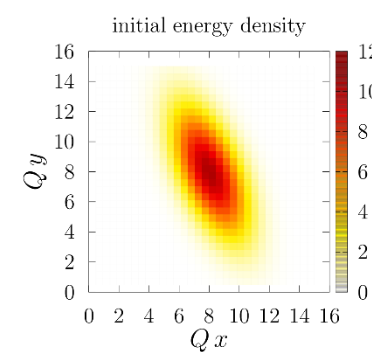

Quark fields

Up to the initial surface $\tau = 0^+$, the Dirac equation under the CGC classical gauge fields can be solved analytically.

Gelis, kajantie, Lappi (2006);
Gelis, Tanji (2016)

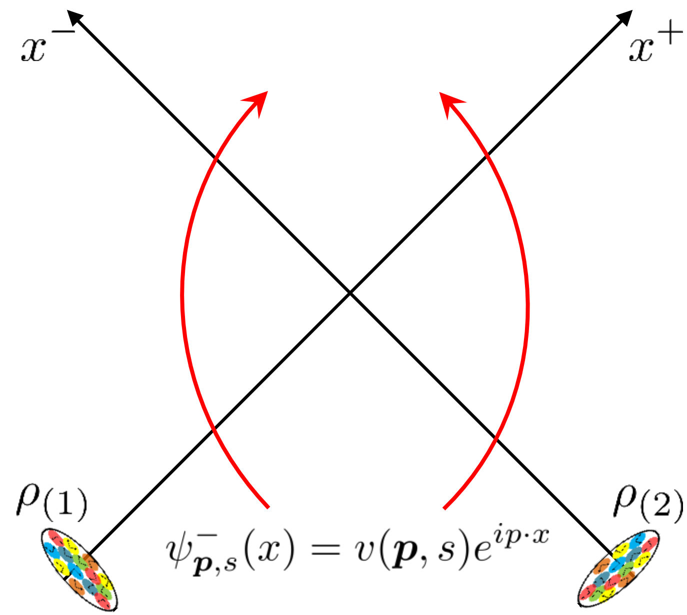

The evolution for $\tau > 0$ can be described by solving the Dirac equation for the mode functions

$$\left(i\gamma^0\partial_\tau + \frac{i}{\tau}\gamma^3 D_\eta + i\gamma^i D_i - m\right)\psi^-_{\boldsymbol{p}_\perp,\nu,s,c}(x) = 0$$

on a real-time lattice in the expanding geometry.

To realize the chiral anomaly on the lattice, we employ the Wilson fermion extended to the expanding geometry.

Tanji, Berges (2018)

Wilson fermion and chiral anomaly

Adler-Bell-Jackiw anomaly equation

$$\partial_\mu j_5^\mu = 2m\langle\overline{\psi}i\gamma_5\psi\rangle + \frac{g^2}{4\pi^2}\boldsymbol{E}^a\cdot\boldsymbol{B}^a$$

Axial current $j_5^\mu = \langle\overline{\psi}\gamma^\mu\gamma_5\psi\rangle$

The Wilson fermion exactly satisfies

$$\partial_\mu j_5^\mu = 2m\langle\overline{\psi}i\gamma_5\psi\rangle + \langle\overline{\psi}i\gamma_5 W\psi\rangle$$

where $W\psi$ is the Wilson term added to the Dirac equation to suppress doublers.

The axial anomaly is realized if

Karsten, Smit (1981)

$$\langle\overline{\psi}i\gamma_5 W\psi\rangle \approx \frac{g^2}{4\pi^2}\boldsymbol{E}^a\cdot\boldsymbol{B}^a$$

which has been confirmed numerically in non-expanding systems.

Tanji, Mueller, Berges (2016);
Mueller, Hebenstreit, Berges (2016);
Mace, Mueller, Schlichting, Sharma (2017)

Anomaly equation in the expanding geometry

ABJ anomaly equation in the τ-η coordinates

$$\frac{1}{\tau}\partial_\tau\left(\tau j_5^\tau\right)+\partial_i j_5^i+\cancel{\frac{1}{\tau}\partial_\eta j_5^\eta}=\cancel{2m\langle\bar{\psi}i\gamma_5\psi\rangle}+\frac{g^2}{4\pi^2}\boldsymbol{E}^a\cdot\boldsymbol{B}^a$$

boost-invariant background $\quad m\approx 0$

Axial charge density per unit transverse are and unit rapidity

$$\begin{aligned}\frac{dN_5}{d^2x_\perp d\eta}&=\tau j_5^\tau(x)\\&=-\int_0^\tau \tau'\partial_i j_5^i\,d\tau'+\frac{g^2}{4\pi^2}\int_0^\tau \tau'\boldsymbol{E}^a\cdot\boldsymbol{B}^a\,d\tau'\end{aligned}$$

Anomaly equation in the expanding geometry

ABJ anomaly equation in the τ-η coordinates

$$\frac{1}{\tau}\partial_\tau\left(\tau j_5^\tau\right) + \partial_i j_5^i + \cancel{\frac{1}{\tau}\partial_\eta j_5^\eta} = \cancel{2m\langle\bar{\psi}i\gamma_5\psi\rangle} + \frac{g^2}{4\pi^2}\boldsymbol{E}^a\cdot\boldsymbol{B}^a$$

boost-invariant background $\quad m \approx 0$

Axial charge density per unit transverse are and unit rapidity

$$\frac{dN_5}{d^2x_\perp d\eta} = \tau j_5^\tau(x)$$

$$= -\int_0^\tau \underbrace{\tau'\partial_i j_5^i}_{\text{diffusion}}\, d\tau' + \frac{g^2}{4\pi^2}\int_0^\tau \underbrace{\tau'\boldsymbol{E}^a\cdot\boldsymbol{B}^a}_{\text{source term}}\, d\tau'$$

- In a uniform system or at very early times, the diffusion term is negligible. Then the axial charge density can be computed solely from the gauge fields. Lappi, Schlichting (2017)
- Otherwise, one needs to solve the Dirac equation.

Uniform Glasma

Take the limit of the flux tube width $\longrightarrow \infty$

Q : typical energy scale of the Glasma

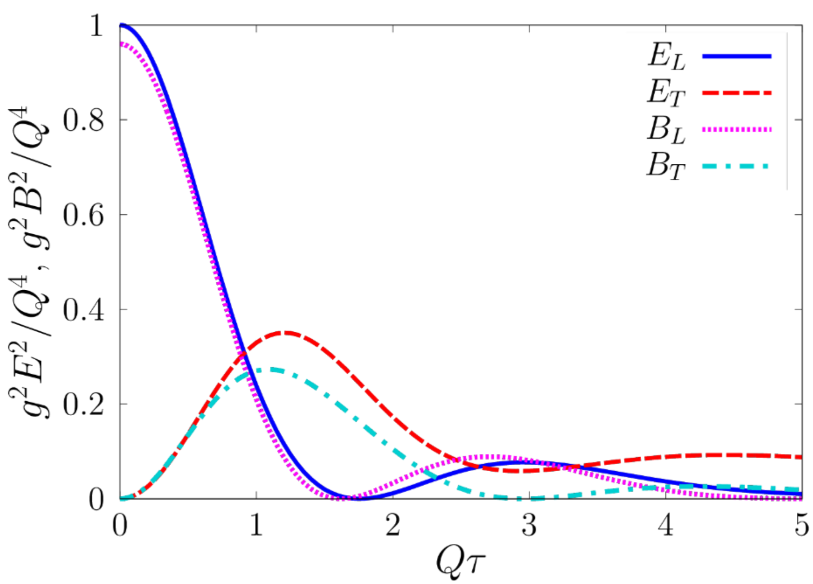

Time evolution of the field strength

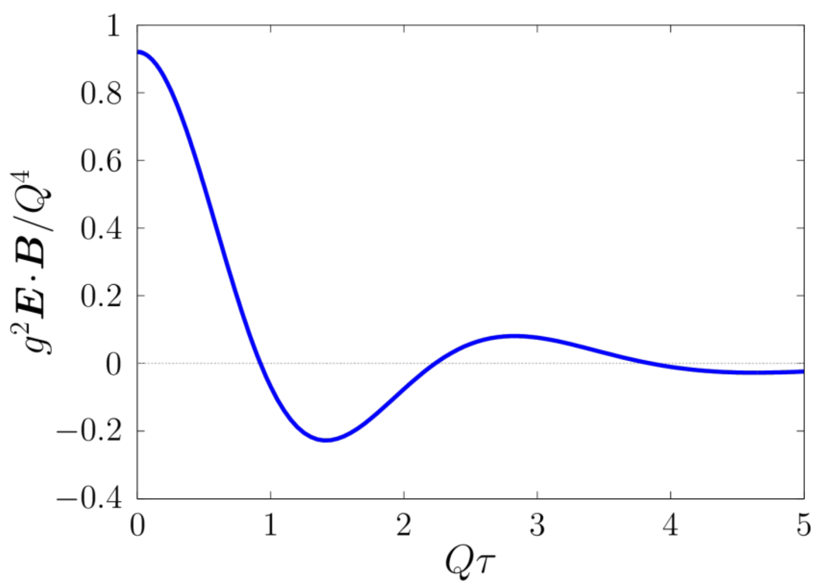

Time evolution of $\boldsymbol{E}\cdot\boldsymbol{B}$

- Similar behavior to that with the MV initial condition.
- In this uniform system, the decay of the fields is a purely nonlinear effect.

Uniform Glasma

$m/Q = 0.01$

$N_x = N_y = 48,\ N_\eta = 512$

Verification of the anomaly relation

$$\frac{dN_5}{d^2x_\perp d\eta} \approx \frac{g^2}{4\pi^2}\int_0^\tau \tau' \boldsymbol{E}^a \cdot \boldsymbol{B}^a \, d\tau'$$

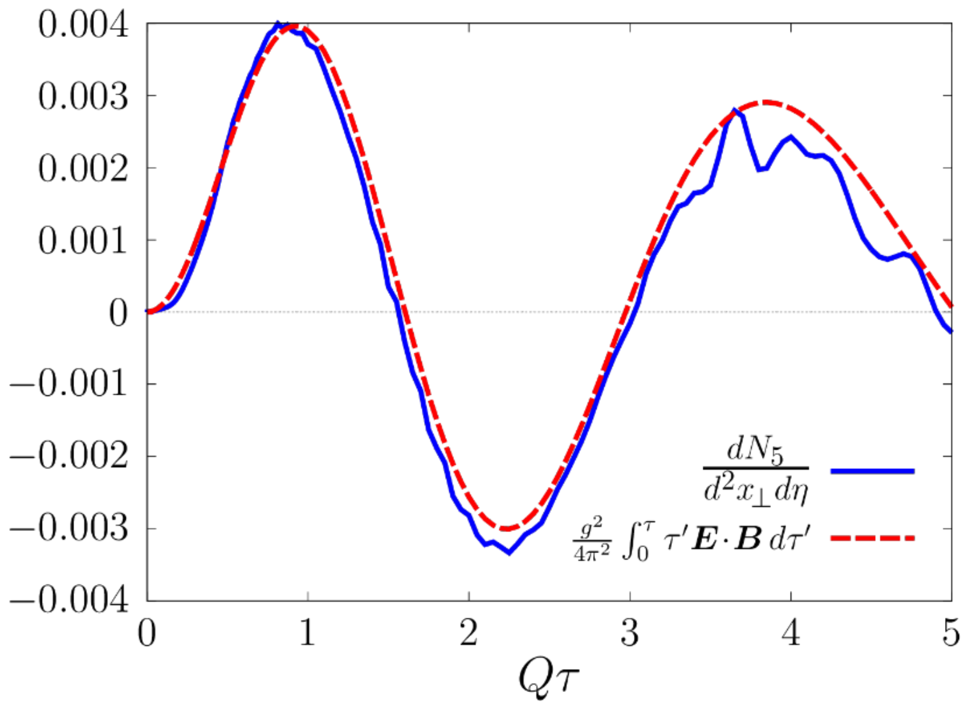

For $Q = 1$ GeV , $\frac{dN_5}{d^2x_\perp d\eta}/Q^2 = 0.04$ $\Longrightarrow$ 1 excess of right-quarks over left-quarks per flavor in a box with 1fm^2 transverse area and one unit of rapidity.

Glasma flux tubes

The profile of flux tubes in the transverse plane

- Two flux tubes to satisfy the periodic b.c.
- Distorted Gaussian to have both E and B.

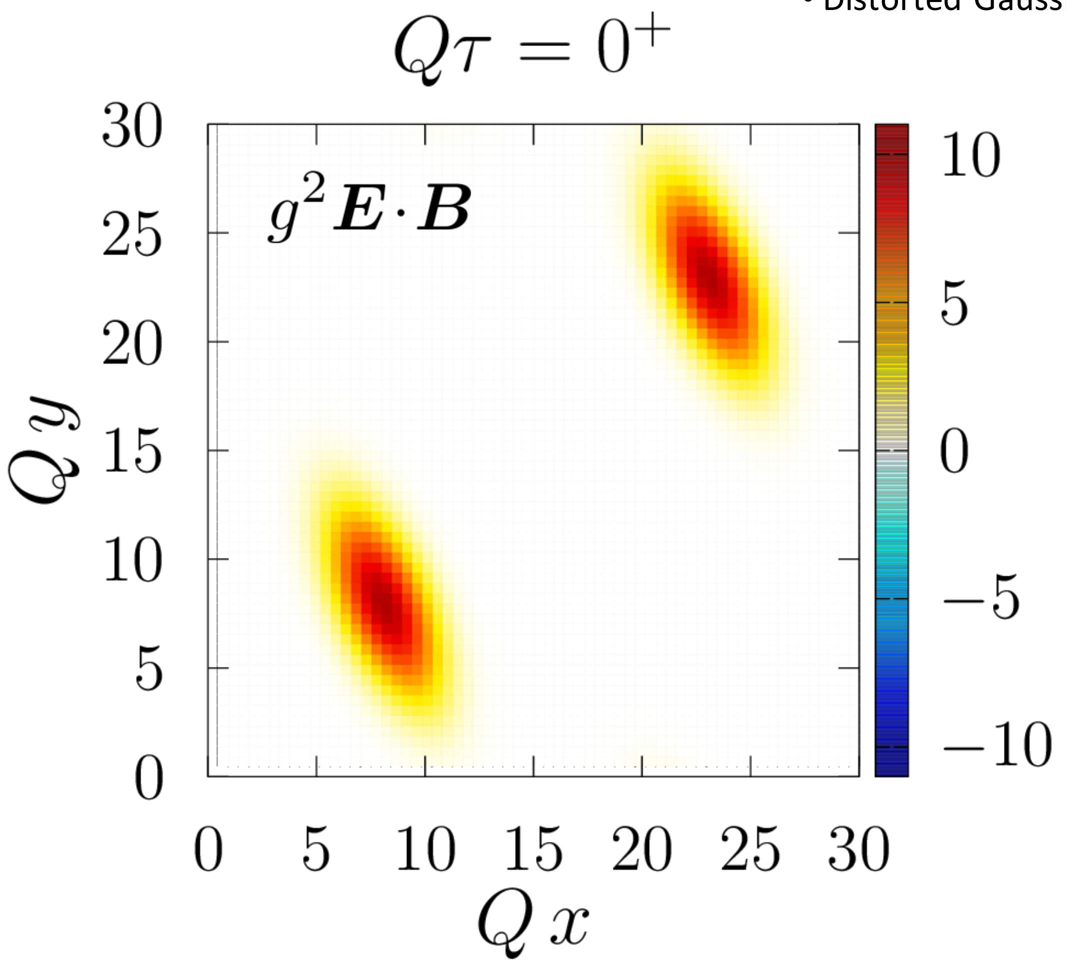

Glasma flux tubes

The profile of flux tubes in the transverse plane

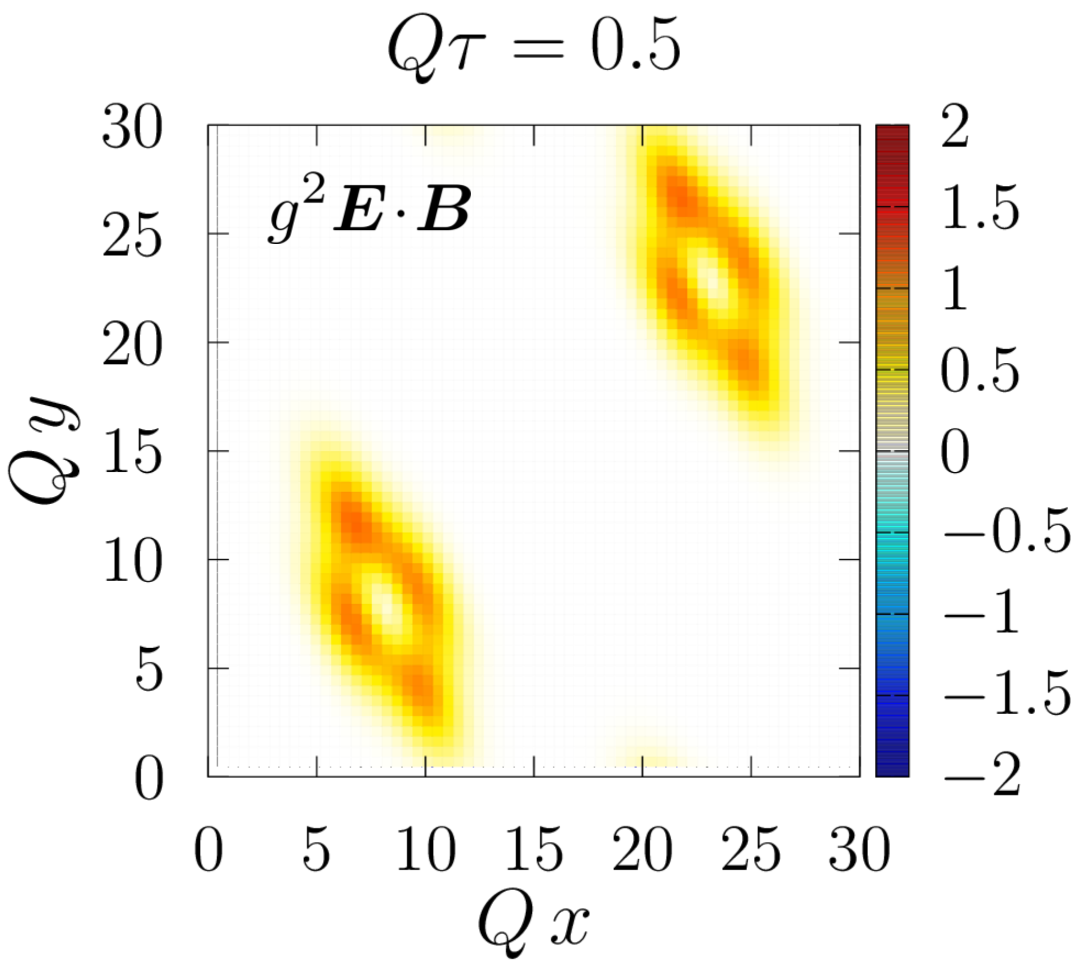

Glasma flux tubes

The profile of flux tubes in the transverse plane

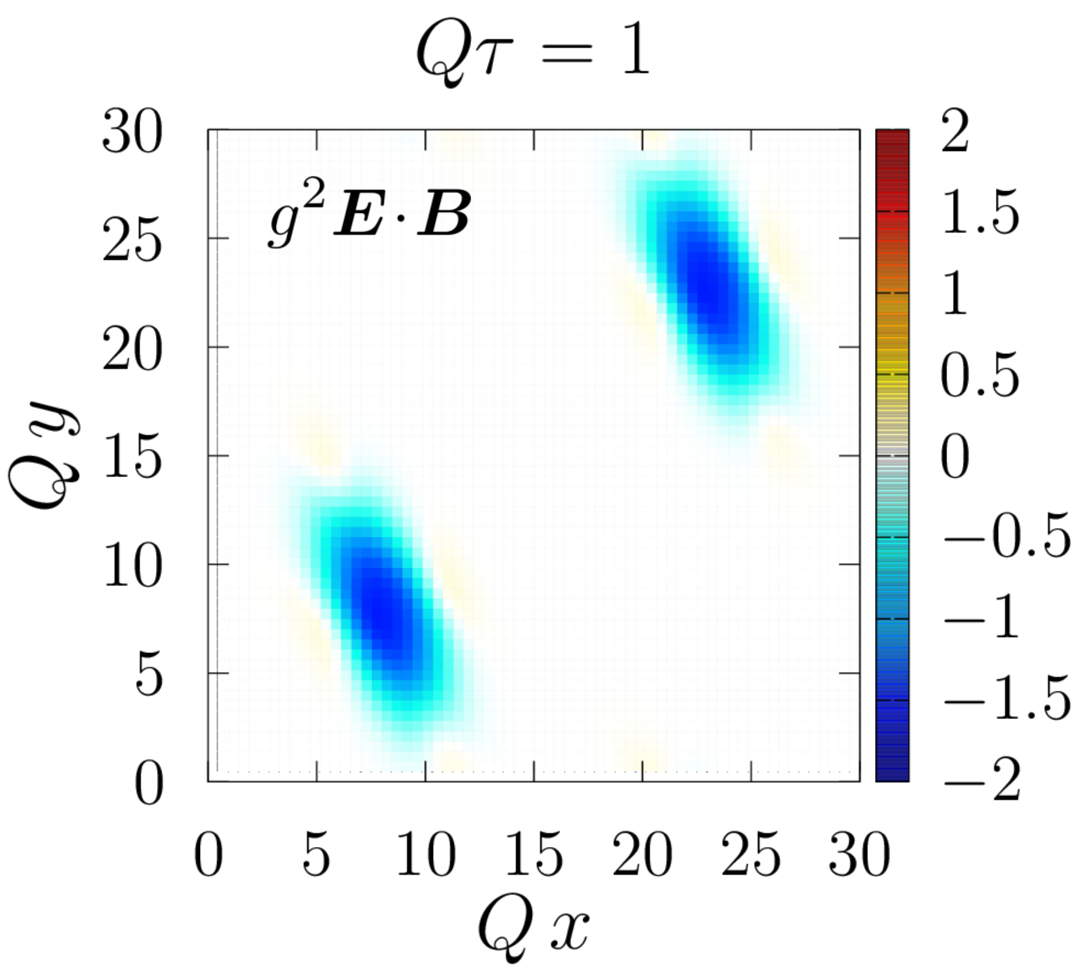

Glasma flux tubes

The profile of flux tubes in the transverse plane

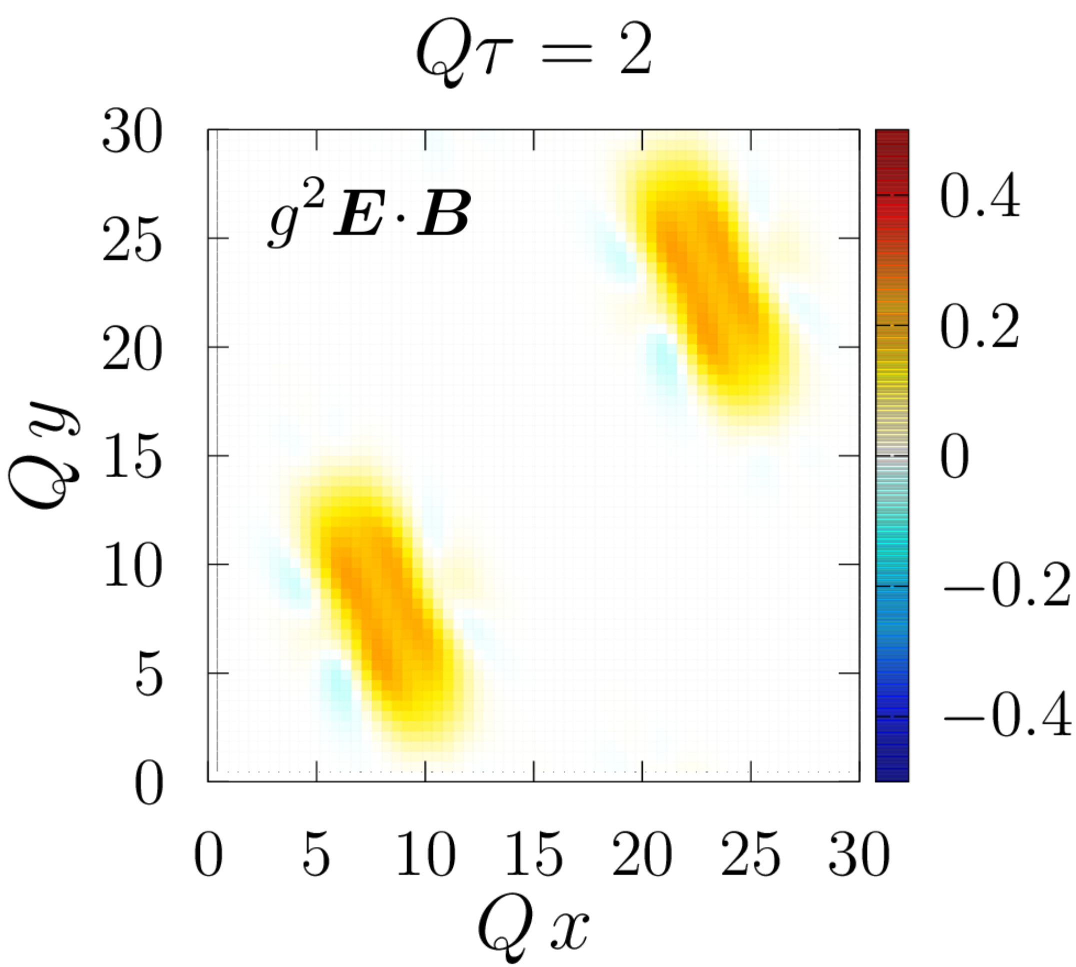

Glasma flux tubes

The profile of flux tubes in the transverse plane

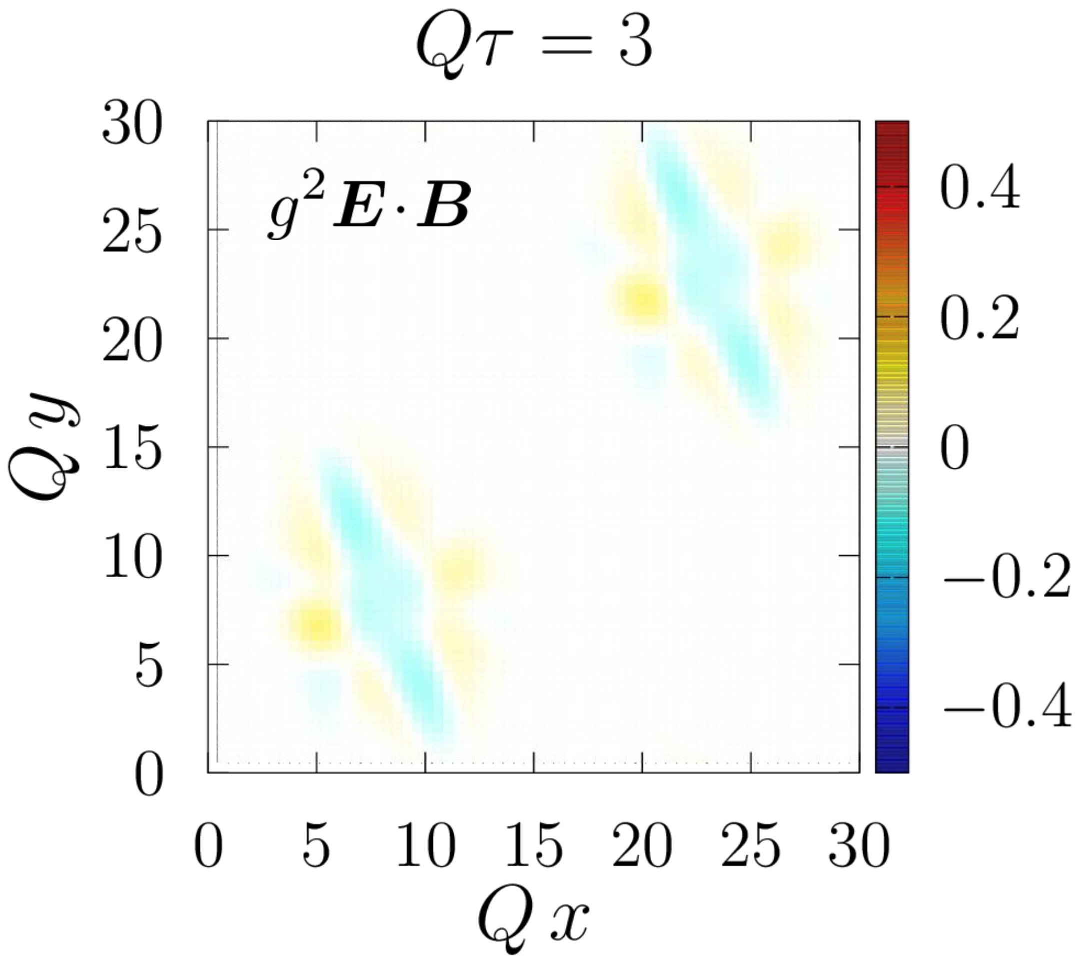

Glasma flux tubes

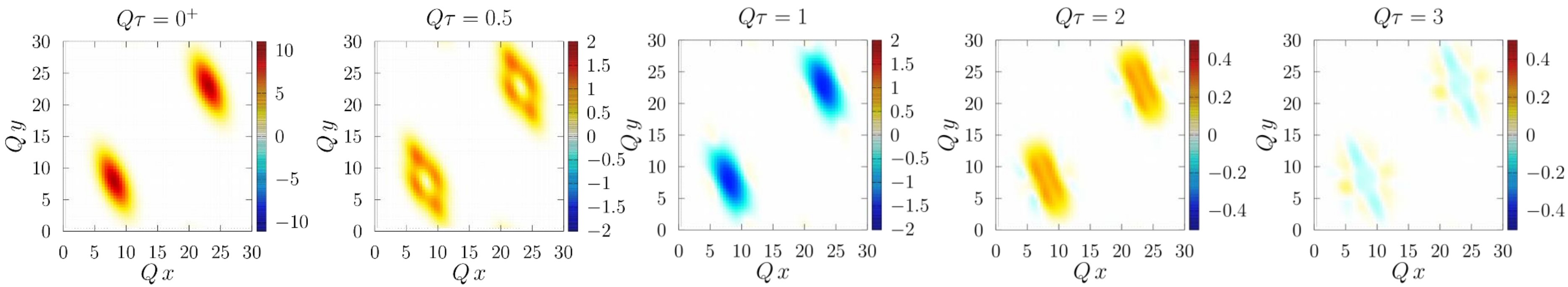

Transverse profiles of $\boldsymbol{E}\cdot\boldsymbol{B}$ for different times

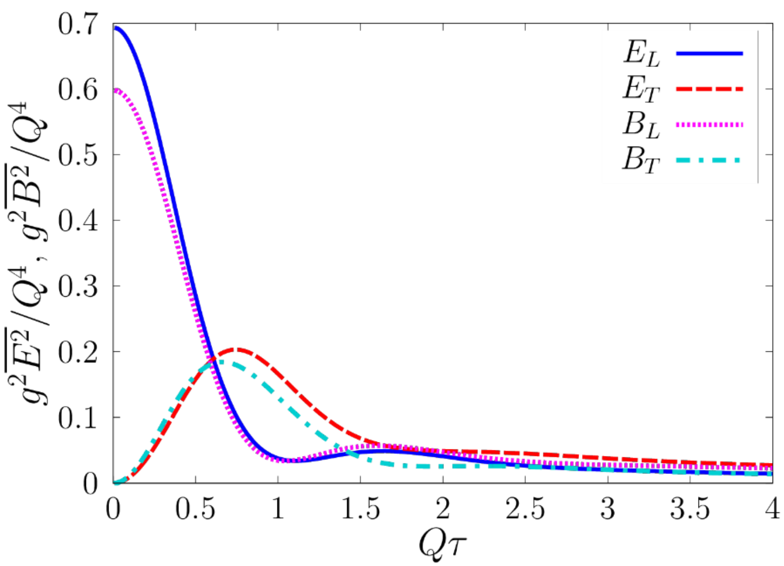

Time evolution of the space-averaged field strength

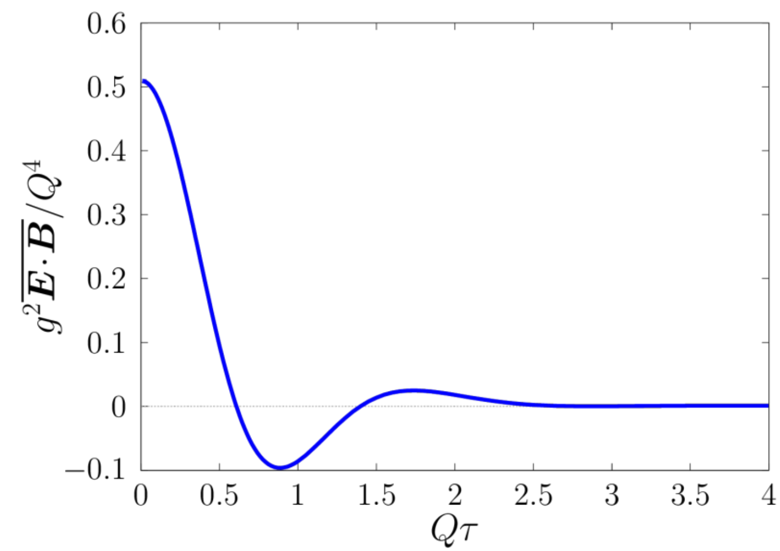

Time evolution of the space-averaged $\boldsymbol{E}\cdot\boldsymbol{B}$

Glasma flux tubes

Verification of the space-averaged anomaly relation

$$\frac{\overline{dN_5}}{d^2x_\perp d\eta} \approx \frac{g^2}{4\pi^2}\int_0^\tau \tau' \overline{\boldsymbol{E}^a \cdot \boldsymbol{B}^a}\, d\tau'$$

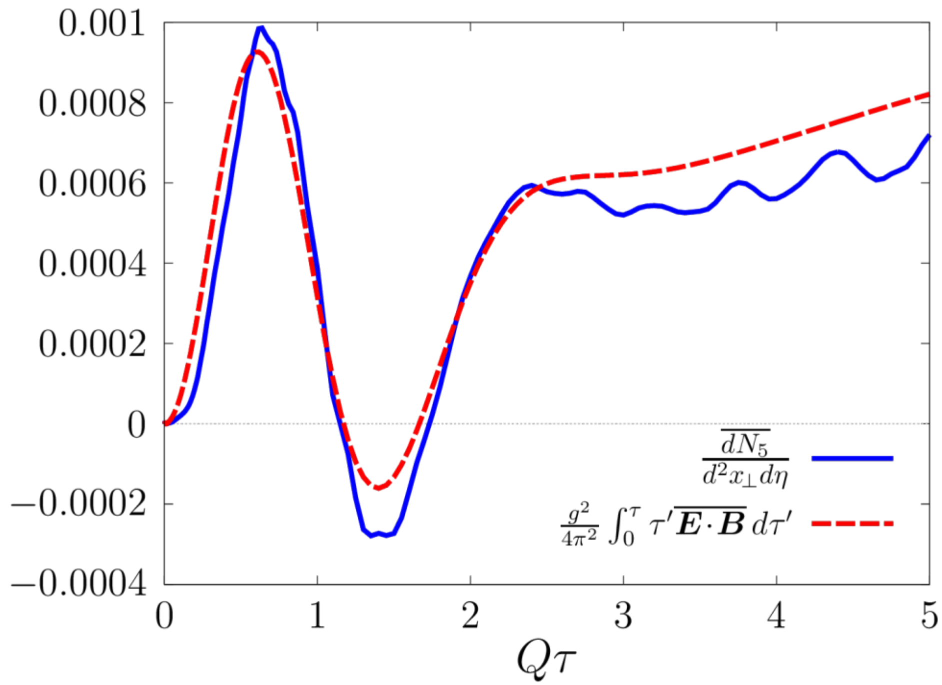

$m/Q = 0.01$

$N_x = N_y = 64,\ N_\eta = 256$

Glasma flux tubes

Verification of the space-averaged anomaly relation

$$\frac{\overline{dN_5}}{d^2x_\perp d\eta} \approx \frac{g^2}{4\pi^2}\int_0^\tau \tau' \overline{\boldsymbol{E}^a\cdot\boldsymbol{B}^a}\, d\tau'$$

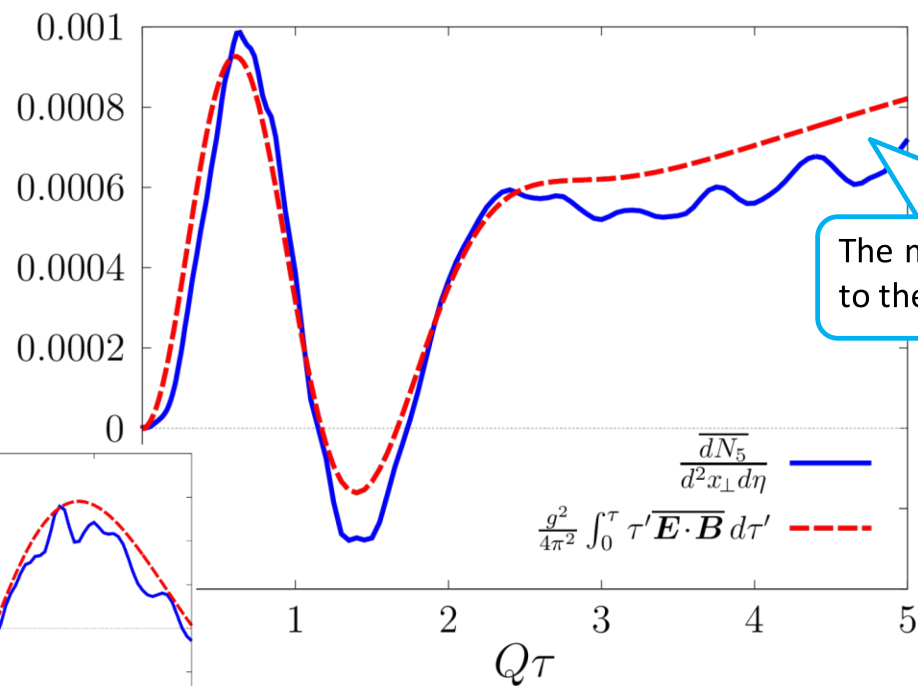

The monotonic increase corresponds to the decaying $\boldsymbol{E}\cdot\boldsymbol{B} \sim 1/\tau$.

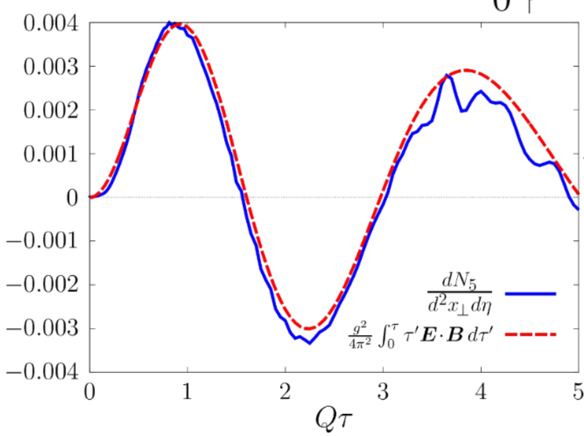

cf. Uniform case

$m/Q = 0.01$
$N_x = N_y = 64,\ N_\eta = 256$

Glasma flux tubes

Local anomaly budget

$$\frac{dN_5}{d^2x_\perp d\eta} + \int_0^\tau \tau' \partial_i j_5^i \, d\tau' \approx \frac{g^2}{4\pi^2} \int_0^\tau \tau' \boldsymbol{E}^a \cdot \boldsymbol{B}^a \, d\tau'$$

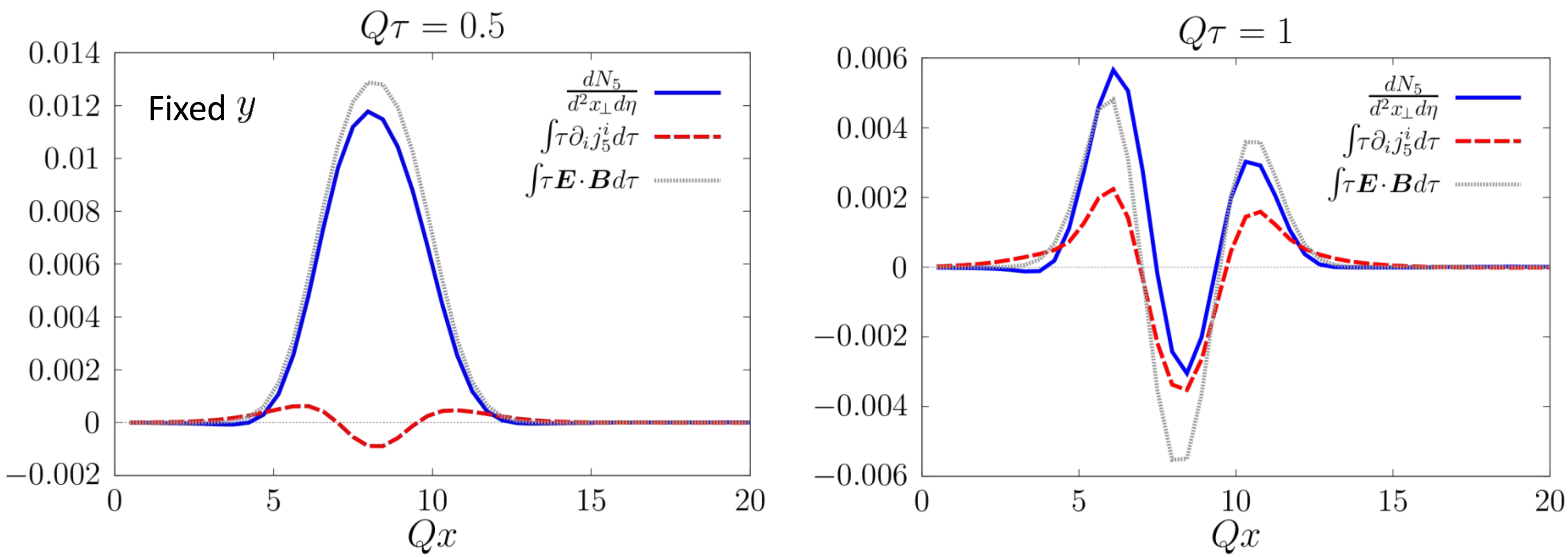

For $Q\tau \gtrsim 1$ the diffusion term takes some fraction of the anomaly budget.

Summary and outlook

- The axial charge production in the longitudinally expanding geometry can be described by the real-time lattice simulations with the Wilson fermion.
- The classical gauge fields having nonzero $\boldsymbol{E}\cdot\boldsymbol{B}$ exhibit nontrivial behaviors.
- Because the axial charge density is related with the time integral of $\boldsymbol{E}\cdot\boldsymbol{B}$, it depends on the time history and it can remain even after $\boldsymbol{E}\cdot\boldsymbol{B}$ dies out.
- In inhomogeneous gauge fields, we need solving the Dirac equation to properly compute the axial charge production including its diffusion dynamics.

  - Real-time simulations of CME in the expanding system by applying a U(1) magnetic field.
  - More realistic configurations?